Journal of Neurochemistry, 2002, **81**, 663–672

Progressive decrease of amyloid precursor protein carboxy terminal fragments (APP-CTFs), associated with tau pathology stages, in Alzheimer's disease

Nicolas Sergeant,* Jean-Philippe David,† Danie Champain,* Antoine Ghestem,* Annick Wattez* and André Delacourte*

**INSERM U422, Lille, France*

†*Centre Hospitalier Emile Roux, Service de Gérontologie Clinique, Limeil Brévannes, France*

Abstract

Amyloid precursor protein (APP) dysfunction is a key aetiologic agent in Alzheimer's disease (AD). The processing of this transmembrane protein generates carboxy terminal fragments (CTFs) upstream of β-amyloid peptide (Aβ) production. The physiologic significance of APP-CTFs is still poorly understood, as well as the relationship that could link APP dysfunction and tau pathology in familial and non-familial AD (non-FAD). In the present study, we have investigated the quantitative and qualitative changes of APP-CTFs in different brain areas of non-demented and demented patients from a prospective and multidisciplinary study. A significant decrease of the five APP-CTFs was observed, which correlated well with the progression of tau pathology, in most cases with infraclinical AD and AD, either familial or non-FAD. Furthermore, solubility properties and the ratio between the five bands were also modified, both in the Triton-soluble and/or -insoluble fractions. Together, we show here for the first time a modification directly observed on APP-CTFs upstream of Aβ products and its relationship with tau pathology, which could reflect the basic aetiological mechanisms of AD.

Keywords: Alzheimer's disease, amyloid precursor protein, pathological tau proteins, proteolytic processing.

J. Neurochem. (2002) **81,** 663–672.

Amyloidosis and neurofibrillary degeneration are the two degenerating processes that characterise Alzheimer's disease. They correspond to dysfunctions of two basic proteins: APP (amyloid precursor protein) and microtubule-associated tau. The amyloid that accumulates in the grey matter of the cortex is composed of heterogeneous β-amyloid peptides (Aβs), which are cleavage products of APP. The enzymes that cleave the APP in the Aβ region are named secretases, with three types of activities in the α, β and γ region (Fig. 1) (De Strooper and Annaert 2000). α-Secretase generates the APPsα and the α-carboxy terminal fragment (CTF). β-Secretase generates the APPsβ, CTFβ and CTFβ′. Aβ peptides and CTFγ result from the cleavage of CTFβ and CTFβ′ by the γ-secretase.

The larger APP-CTFs containing the entire sequence of Aβ are neurotoxic, as demonstrated in cell or in animal models (for a review see Suh 1997). Furthermore, they could have physiologically important roles resulting from their interaction with numerous adaptor proteins such as Fe65, suggested for control of gene expression (Cao and Sudhof 2001), or signalling proteins such as X11L (Neve *et al*. 2000; Neve 2001).

Little is known about the fate of APP-CTFs at the different stages of AD, as well as their precise relationship with amyloid and tau pathologies. The aim of this work was essentially to determine if these fragments are modified in non-familial AD (non-FAD), and to investigate their potential link with the markers of neurodegeneration. Tools at our disposal were an important bank of frozen brain tissue from non-demented and demented Alzheimer patients, from a prospective and multidisciplinary study, and reliable immunological probes against APP-CTFs.

Received November 27, 2001; revised manuscript received December 13, 2001; accepted January 3, 2002.

Address correspondence and reprint requests to André Delacourte, INSERM U422, 1 Place de Verdun, 59045 Lille Cedex, France.
E-mail: delacourte@lille.inserm.fr

Abbreviations used: AD, Alzheimer's disease; APP, amyloid precursor protein; CTF, carboxy terminal fragment; FAD, familial AD; IP, immunoprecipitation; infra-AD, infraclinical non-FAD; IPG, immobilized pH gradient; NSE, neurone-specific enolase; PAGE, polyacrylamide gel electrophoresis; SDS, sodium dodecyl sulfate.

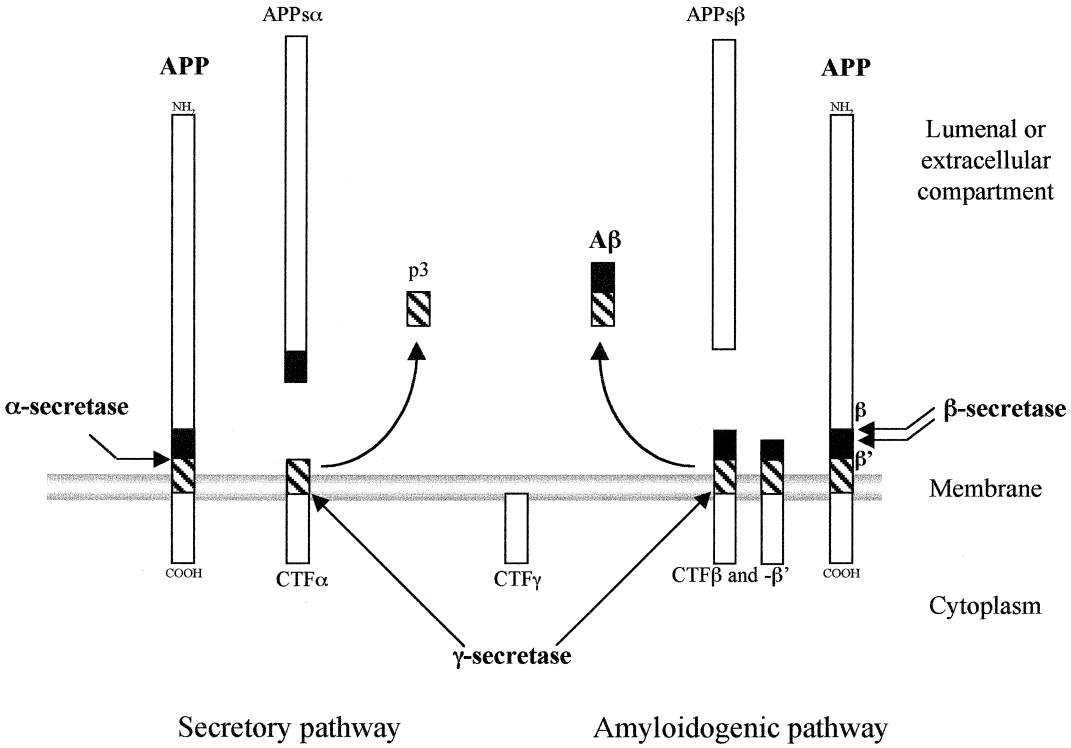

Fig. 1 Schematic summary of APP processing. The non-amyloidogenic or secretory pathway is represented on the left. It results from the cleavage of APP inside the Aβ sequence by the α-secretase and generates the secreted from of APP, named APPsα, and the carboxy terminal fragment (CTFα). The amyloidogenic pathway leading to Aβ peptide is represented on the right. The β-secretase cleaves APP at the amino-terminus of Aβ giving a secreted form, named APPsβ and carboxy terminal fragment (CTFβ). The β′ site of cleavage is also described at position 11 of Aβ. The γ-secretase generates Aβ by cleaving the CTFβ at the carboxy terminus of Aβ and releases the carboxy terminal fragment (CTFγ).

Materials and methods

Patients

We included 130 cases in the present study. Most of the samples from aged non-demented patients ($n = 60$) and several demented patients ($n = 35$) were obtained from the geriatric department of E. Roux Hospital (Limeil-Brevannes, France) and the Department of Neurology of the University Hospital Centre (Lille, France). The clinical assessments and neuropathology were already described (Delacourte *et al*. 1999). The post-mortem times ranged from 5 h to 61 h. The human brain biopsy sample was obtained from a tumour resection directly frozen in liquid nitrogen and kept at −80°C until biochemical analysis. Clinical and neuropathological data from patients are indicated in Table 1. This study included non-FAD cases ($n = 14$, age 75 ± 13 years), infraclinical non-FAD cases (infra-AD; $n = 9$, age 84 ± 10) and control subjects (Ctrl; $n = 7$, age 54 ± 18) (Table 1). Two patients with familial Alzheimer's disease caused by PS1 mutation (Campion *et al*. 1996), FAD 1 codon 235 and FAD 2 codon 163, were included in this study.

Antibodies

Two New Zealand rabbits were immunized with a synthetic peptide corresponding to the last 17 amino acids of the human APP sequence. The serum was directly used or purified by affinity chromatography with the peptide covalently coupled to NHS-Sepharose. This antibody is named APPCter-C17. The B10 antiserum (a kind gift from Bart De Strooper, Leuven, Belgium) is raised against the C-terminal region of APP (De Strooper *et al*. 1995). A lab-made specific monoclonal antibody against the neurone-specific enolase (NSE), named 1C1, was used as neuronal marker. Briefly, 1C1 detects a single band at 47 kDa on brain tissue homogenates. Using two-dimensional gel electrophoresis followed by western blotting, it was shown to react with a single spot at 47 kDa, the isoelectric point of 4.9. This spot was isolated and analysed by mass spectrometry and it matched with the γ-enolase or NSE. WO2 monoclonal antibody (Abeta, GmBH, Heidelberg, Germany) is raised against the amino-terminal region of Aβ and reacts strongly with APP fragments that contain the sequence 4–10 of Aβ (Fassbender *et al*. 2001). Anti-mouse or anti-rabbit antibodies coupled with horseradish peroxidase were purchased at SIGMA Immunochemicals (Saint Quentin Fallavier, France).

Brain tissue samples preparations and immunoprecipitation

Tissues were homogenized using a Teflon potter in 10 volumes of Laemmli sample buffer containing 5% (w/v) sodium dodecyl sulfate (SDS) and boiled for 10 min. For fractionation experiments, the cortical brain samples were homogenized in 10 volumes of 10 mM Tris-HCl pH 6.8 buffer and centrifuged at 100 000 *g* for 1 h. The supernatants (fractions F1) were collected, the pellets were re-suspended in Tris buffer containing 1% (v/v) of Triton X-100

Table 1 Clinical and biochemical data of the patients included in the study

	(2)															
	Hippocampal reg			Temporal ctx.			Frontal ctx			Occ. ctx					(6)	
(1)												(3)	(4)	(5)	Homo-	
Cases	*A35*	*Ent*	*CA1*	*A38*	*A20*	*A21*	A10	*A44*	*A4*	*A18*	*A17*	Amyloid	CERAD	CEBDAD	genate	F2	F3
B0,a												0	control	control	→		
S0,a												0	control	control	→	→	→
S0,b												0	control	control	→	→	→
S0,c												0	control	control	→	→	→
S0,d												0	control	control	→	→	→
S0,e												0	control	control	→	→	→
S1,a	■											+	control	IAD	→	→ / DE↑	→
S2,a	■	■										0	control	control	→	→	→
S2,b	■	■										+	control	IAD	↓		
S3,a	■	■	■									+	control	IAD	↓	→ / DE↑	↓ / AB↑
S3,b	■	■	■									+	control	IAD	→	→ / DE↑	→
S3,c	■	■	■									+	control	IAD	→	→ / DE↑	→
S4,a	■	■	■	■								+	control	IAD	↓	↓	↓
S5,a	■	■	■	■	■							+	control	IAD	↓		
S6,a	■	■	■	■	■	■						+	memory impt	IAD	↓		
S6,b	■	■	■	■	■	■						+	memory impt	IAD	↓		
S7,a	■	■	■	■	■	■	■					+	probable AD	AD	↓		
S7,b	■	■	■	■	■	■	■					+	vascular dementia	AD	↓	↓ / DE↑	↓ / AB↑
S8,a	■	■	■	■	■	■	■	■				+	probable AD	AD	↓		
S9,a	■	■	■	■	■	■	■	■		■		+	probable AD	AD	↑	↑ / DE↑	↑ / AB↑
S9,b	■	■	■	■	■	■	■	■		■		+	probable AD	AD	→	→ / DE↑	→ / AB↑
S9,c	■	■	■	■	■	■	■	■	■	■		+	possible AD	AD	↓		
S9,d	■	■	■	■	■	■	■	■	■	■		+	probable AD	AD	↓	↓	0
S9,e	■	■	■	■	■	■	■	■	■	■		+	probable AD	AD	↓	↓	↓
S9,f	■	■	■	■	■	■	■	■	■	■		+	probable AD	AD	↓		
S10,a	■	■	■	■	■	■	■	■	■	■	■	+	probable AD	AD	↓	↓ / DE↑	→
S10,b	■	■	■	■	■	■	■	■	■	■	■	+	probable AD	AD	→	↓ / DE↑	→ / AB↑
S10,c	■	■	■	■	■	■	■	■	■	■	■	+	probable AD	AD	↓	↓ / DE↑	→
S10,d	■	■	■	■	■	■	■	■	■	■	■	+	probable AD	AD	↓	↓ / DE↑	→
S10,e	■	■	■	■	■	■	■	■	■	■	■	+	probable AD	AD	↓		
FAD 1	■	■	■	■	■	■	■	■	■	■	■	+	FAD (PS1 mut235)	AD	↓		
FAD 2	■	■	■	■	■	■	■	■	■	■	■	+	FAD (PS1 mut235)	AD	↓		

(1) Patients ($n = 32$) are ranked as a function of tau pathology stages. (2) The extent of tau pathology in the different brain areas is mentioned and the brain areas affected are indicated ■. (3) The presence (+) or absence (0) of an amyloid burden, detected at the neuropathological and biochemical level is indicated. (4) The main clinical data are summarized. (5) The final diagnosis was based upon the biochemical amounts of $^{A\beta}$ and tau in the different brain areas (CEBDAD; Delacourte *et al.* 1999). (6) The main APP-CTFs changes in total brain tissue homogenates, F2 (Triton-soluble) and F3 (Triton-insoluble) brain extracts are indicated. ↓ Decreased, → not modified, ↑ increased, APP-CTFs; AB and DE specifies the bands that are specifically modified. 0, APP-CTFs were totally absent.

and centrifuged at 100 000 *g* for 1 h. The supernatants (fractions F2) were collected and the pellets (fractions F3) were homogenized in Laemmli sample buffer.

For immunoprecipitation (IP) experiments, 100 μL of the F2 fraction were diluted in three volumes of IP buffer containing 10 mM Tris-HCl pH 7.4, 150 mM NaCl, 1% (v/v) NP-40 and EDTA-free protease cocktail inhibitors (Roche Molecular Biochemicals, Meylan, France) and pre-cleared with 10 μL of Immunopure® protein A-agarose (Pierce, Bezons, France) for 1 h at 4°C. Following centrifugation at 7000 *g*, the supernatant was added with 10 μL of APP-CterC17 antiserum and incubated overnight at 4°C. Immunopure® protein A-agarose (40 μL) was added and incubated for 1 h at 4°C. Agarose beads were washed three times with the IP buffer and 50 μL of non-reducing Laemmli sample buffer was added and incubated at 60°C for 5 min prior to centrifugation at 7000 *g*. The supernatant was collected for western blot analyses.

Treatment of immunoprecipitated APP-CTFs with calf intestine alkaline phosphatase (EC 3.1.3.1; Molecular Roche Biochemicals) was performed according to the manufacturer's instructions. Briefly, following IP, agarose beads were washed three times with IP buffer, 50 μL of calf alkaline phosphatase buffer and 400 U/mL of enzyme was added and incubated at 37°C overnight. The reaction mixture was centrifuged at 7000 *g*, the supernatant discarded and 50 μL of non-reducing Laemmli sample buffer was added, as was done for the IP experiments. In a control experiment, immunoprecipitated APP-CTFs were processed without the addition of the enzyme.

Western blot analyses

All protein samples were processed in Laemmli sample buffer and the same quantity of total brain proteins (100 μg/lane) was loaded on a 16.5% polyacrylamide gel. Tris-Tricine SDS–polyacrylamide gel electrophoresis (PAGE) was performed following the procedure of Schägger and von Jagow (1987) with a Protean II Xi Cell (Bio-Rad Laboratories, Hercules, CA, USA). Following electrophoresis, proteins were transferred to nitrocellulose membrane at 2.5 mA/cm^2 per gel using the semidry Novablot transfer system (Amersham Pharmacia Biotech, Piscataway, NJ, USA), according to the manufacturer's instructions. Proteins were reversibly stained with Ponceau Red to check the quality of the transfer. Membranes were blocked in 25 mM Tris-HCl pH 8.0, 150 mM NaCl, 0.1% Tween-20 (v/v) and 5% (w/v) of skimmed milk for 1 h. Membranes were incubated overnight at 4°C or 2 h at room temperature with appropriate dilutions of the primary antibodies, and incubated for 1 h at room temperature with secondary antibody. The immunoreactive complexes were revealed using the ECL western blotting kit (Amersham Pharmacia Biotech) on Hyperfilms (Amersham Pharmacia Biotech).

For two-dimensional gel electrophoresis, 400 μg of protein was loaded on immobilized pH gradient (IPG) strip 3–10 (Bio-Rad), isoelectrofocalization was performed with the Protean IEF Cell System (Bio-Rad) applying a total of 75 kV/h, according to the manufacturer's instructions (Westermeier *et al*. 1983; Gorg 1993). The IPG-strip was equilibrated three times for 10 min in Laemmli sample buffer and was disposed over a 16.5% Tris-Tricine SDS–PAGE.

Quantification and statistical analysis of data

Western blots films were digitized using an Umax scanner calibrated for optical densities (Amersham Pharmacia Biotech). The IMAGE-MASTER 1D ELITE software (Amersham Pharmacia Biotech) was used to quantify the signal, and data were collected using EXCEL software (Microsoft, LesUlis, France). Statistical analyses were performed with STATVIEW software (StatView SE+Graphics™, Abacuc Concept Inc., Meylan, France).

Results

Carboxy terminal proteolytic products of APP in human brain tissue

The specificity of APPCter-C17 antiserum was compared with the purified antiserum B10 (De Strooper *et al*. 1995) (Fig. 2a, lane 1). The same electrophoretic profile was observed, consisting of five individual bands ranging from 8 to 15 kDa (Fig. 2a, lane 2) as previously described (Estus *et al*. 1992; Golde *et al*. 1992; Haass *et al*. 1992; LeBlanc 1994; Russo *et al*. 2001). These APP-CTFs bands were detected by the purified antiserum APPCter-C17, whereas the absorbed serum collected after affinity chromatography showed no immunoreactivity (Fig. 2a, lane 3). Thus, the five bands A–E correspond to human APP-CTFs. Moreover, in biopsy derived human brain tissue, the five APP-CTFs were detected with the same electrophoretic profile as that observed in autopsy brain tissue homogenates, demonstrating that none of the APP-CTFs are generated during post-mortem delays (Fig. 2b).

A quantitative analysis of APP-CTFs was performed in control, infra-AD, AD and FAD (PS1 mutation) total brain tissue homogenates (Figs 2b and c). Infra-AD patients correspond to non-demented patients, with an important amyloidosis and tau pathology (Table 1), as defined in Delacourte *et al*. (1999). The five APP-CTFs bands were detected with a similar pattern in control, infra-AD, AD and FAD brain tissue homogenates (Figs 2b and c). However, a reduced signal of APP-CTFs was observed in the infra-AD and AD cases, as well as in FAD when compared with the control cases. In contrast, APP holoprotein was observed with similar expression profile even in the brain tissue with important loss of APP-CTFs (Fig. 2b). Statistical analysis showed that the decrease in the quantity of APP-CTFs was 1.5-fold ($p < 0.03$) for the infra-AD and 1.7-fold ($p < 0.002$) for AD (Fig. 3a). Intriguingly, among the AD patients analysed an increase of APP-CTFs of 1.5-fold was observed, but this was for one AD case exclusively (Fig. 2b, AD lane 5; Fig. 3a, ○). Overall, our results show a significant decrease in the quantity of APP-CTFs in non-FAD and FAD cases (Fig. 3a).

Relationship between APP-CTFs reduction and tau pathology stages in AD

At least one patient per stage of tau pathology was studied among the patients included in the present study. The quantity of APP-CTFs was compared with the stages of tau

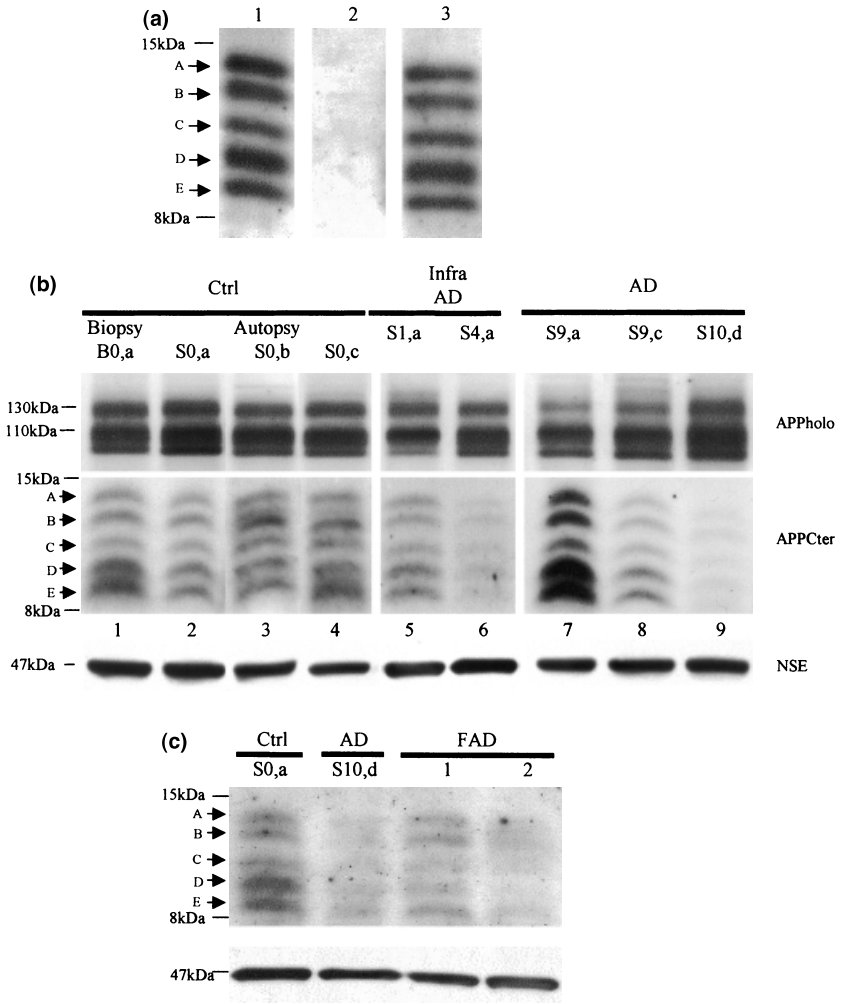

Fig. 2 Analysis of APP-CTFs in control and AD brain tissues. (a) Western blot analysis of a control brain homogenate with antibodies against carboxy terminal fragments of human APP. Immunodetection with APPCter-C17 (lane 1) and with B10 (lane 3). The immunodetection was completely abolished following adsorption of APPCter-C17 with the C17 synthetic peptide (lane 2). (b) Analysis of APP holoprotein, APP-CTFs and NSE expression in total human brain tissue homogenates of the temporal cortex of controls (a biopsy and three autopsy samples), of infra-AD and AD patients. APP holoprotein, APP-CTFs and NSE were detected with APPCter-C17 antiserum and 1C1 antibody, respectively. APP holoproteins were resolved as three bands between 100 and 130 kDa. Similar quantities of APP holoproteins are observed in the cases studied. Five major bands of APP-CTFs (A–E) migrating between 8 and 15 kDa were detected in all cases. NSE, used as an internal neuronal marker, was detected as a single band at 47 kDa. Different quantities of APP-CTFs were detected in infra-AD and AD cases, compared with controls. APP-CTFs were decreased in some infra-AD patients (lane 6); exceptionally increased in AD (one patient, lane 7), normal in a few infra-AD and AD patients (lane 5 and lane 8) and frequently decreased in AD patients (lane 9). (c) APP-CTF levels detected in two samples of FAD (familial autosomic dominant AD) caused by PS1 mutations, compared with control (case S0,a) and an AD patient (case S10,d). A decrease of APP-CTFs immunoreactivity is generally observed in all Alzheimer patients compared with controls.

pathology that reflect well the progression of the disease (Delacourte *et al.* 1999). Significant correlation was observed between the level of APP-CTFs and the progression of tau pathology in the temporal ($p < 0.0001$) and in the occipital cortex ($p < 0.003$) (Fig. 3b and statistics table). No correlation was found between the APP-CTFs modifications and other known factors such as age, sex, ApoE genotype and post-mortem delay (data not shown).

Modification of the solubility distribution of APP-CTFs

To investigate further the APP-CTFs in the human brain, a solubility fractionation of APP-CTFs was performed as already described (Allinquant *et al.* 1994; Bouillot *et al.* 1996; Ikezu *et al.* 1998; Hayashi *et al.* 2000). In control brain tissue, the first Tris-buffer fraction (F1) did not contain APP-CTFs (Fig. 4a, F1). A large quantity of APP-CTFs was extracted in fraction F2, in 1% of non-ionic detergent

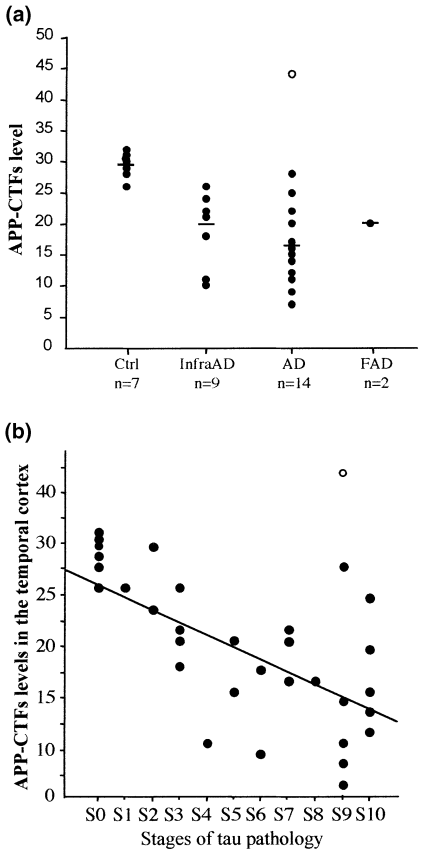

Linear regression

	n	r	p
Temporal cortex	30	0.698	0.0001
Occipital cortex	26	0.616	0.003

Fig. 3 APP-CTFs and tau pathology. (a) APP-CTFs levels in the temporal cortex from four groups: Control cases (Ctrl), infraclinical AD cases (infra-AD), AD cases (AD) and familial AD cases (FAD). A significant decrease was observed between infra-AD and AD vs. Ctrl (IAD, $p < 0.007$; AD, $p < 0.001$), using the non-parametric statistic test of Mann–Whitney. Average decrease of APP-CTFs was of 1.5-fold for infra-AD and of 1.7-fold for AD vs. controls. Patient S9,c (○) had a 1.5-fold increase of APP-CTFs. The decrease of APP-CTFs in the infra-AD and AD groups was not significantly different. (b) Linear regression between APP-CTFs levels and tau pathology in human temporal cortex of patients at different stages of tau pathology. A significant relationship was observed between APP-CTFs levels in the temporal cortex and in the occipital cortex of each patient studied and the different stages of tau pathology in AD (statistics table).

Triton X-100, and no additional APP-CTFs were detected after a repeated extraction in the same conditions (Fig. 4a, F2′). The third fraction (F3) was recovered in Laemmli sample buffer. The five APP-CTFs bands were detected in both fractions F2 and F3 without any differential solubility between APP-CTFs bands, and more than 50% were recovered in the F2 fraction (Fig. 4a).

The same approach was used to analyse the differential solubility distribution of APP-CTFs in control, infra-AD and AD cases (Fig. 4b). Temporal and occipital regions were analysed and showed similar results (shown for temporal region). Modifications of APP-CTFs were observed in F2 and F3 fractions in infra-AD and AD cases when compared with control cases. Indeed, the labelling was more intense for APP-CTFs bands D and E in F2 fraction in infra-AD and in AD cases (Fig. 4b and Table 1). In F3 fraction, APP-CTFs bands A and B were increased in AD patients. In infra-AD and AD cases with a decreased quantity of APP-CTFs, the decrease was stronger in the F3 fraction (Fig. 4b, lanes 6 and 8 of infra-AD and AD). The increase was observed in F2 and F3 fractions (Fig. 4b, AD lane 9) in the only AD case showing a global increase in APP-CTFs (Fig. 3a, ○). However, as for infra-AD and AD cases, in the F2 fraction APP-CTFs bands D and E were more intensively labelled, and in the F3 fraction the APP-CTFs bands A and B staining was stronger. APP-CTFs are therefore qualitatively modified in infra-AD and AD when compared with control, even at the early stages of AD (stages 1–3) where the global quantity of APP-CTFs was not significantly decreased.

We also investigated if the decrease of APP-CTFs was the result of a complete insolubilization, as observed for Aβ aggregation into totally SDS-insoluble aggregates (Delacourte *et al.* 1999). For that purpose, we solubilized the brain tissue with progressive concentrations of formic acid, and then we neutralized and dissolved the brain tissue homogenate in SDS buffer for SDS–PAGE analysis. Aβ peptides were released using this method but no additional quantity of APP-CTFs was recovered (data not shown).

Characterization, phosphorylation and two-dimensional analysis of APP-CTFs

To further characterize the APP-CTFs bands, an immunostaining was performed with WO2 antibody that recognizes the amino-terminal region of Aβ as well as APP fragments including this sequence (Ida *et al.* 1996; Fassbender *et al.* 2001). Thus, the use of WO2 would enable us to distinguish between β-stub and β′-, α- and γ-stubs. Following IP with APPCter-C17, APP-CTFs bands A and B were detected with WO2 showing that they both correspond to β-stubs fragments (Fig. 4c). Consequently, APP-CTFs bands C, D and E might correspond to β′-, α- and γ-stubs. Alkaline phosphatase treatment of IP APP-CTFs reduced the number of bands from five to three (Fig. 4d). APP-CTFs bands A and C disappeared, whereas a stronger signal was observed for bands B and E. These results suggest that band B and band E correspond to the unphosphorylated β-stub and α-stub, respectively. Conversely, band A corresponds to phosphorylated β-stub. The dephosphorylated band D could

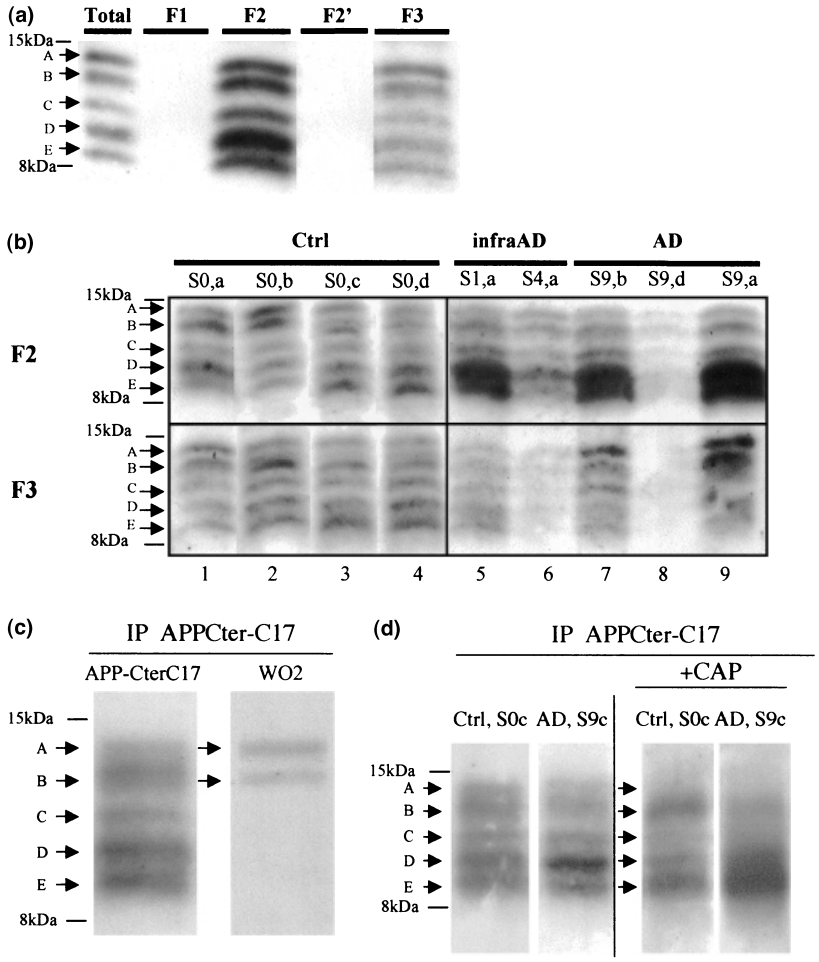

Fig. 4 Differential solubility, characterization and dephosphorylation of APP-CTFs. (a) Brain tissue from a control case was homogenized at a ratio 1 : 10 in Tris-buffer and centrifuged as described in Materials and methods. The supernatant corresponds to fraction F1. The pellet was homogenized in Tris-buffer with Triton X-100 and centrifuged. A second extraction in the same buffer was performed and the supernatant corresponds to fractions F2 and F2′, and the resulting pellet was homogenized in Laemmli sample buffer (fraction F3). Protein from each fraction (50 μg) was loaded on Tris-Tricine SDS–PAGE and APP-CTFs (indicated by arrows) were detected with the APPCter-C17 antiserum. Note that more than 50% of APP-CTFs are soluble in Triton X-100 and the insoluble counterpart is detected in the fraction F3. (b) Different patterns of APP-CTFs in the Triton and SDS fractions. APP-CTFs (indicated by arrows) were analysed in fractions F2 and F3 of 4 controls (Ctrl), two infraclinical AD (infra-AD) and three AD cases. A longer exposure is presented for fraction F3. Note – the decrease of APP-CTFs, essentially in the F3 fraction; – the preferential increase of detection of APP-CTFs bands D and E in fraction 2 of some infra-AD and AD (lanes 5, 7 and 9); – the preferential increase of bands A, B in fraction F3 of some AD patients (lanes 7 and 9). The AD case lane 9 corresponds to the patient showing a global higher expression of APP-CTFs. (c) APP-CTFs from the F2 fraction of control case S0,c (temporal cortex) were immunoprecipitated and revealed with WO2 antibody. Note that the five APP-CTFs bands are detected with APP-CterC17 antiserum following immunoprecipitation with the same antiserum (lane APP-CterC17), whereas WO2 antibody detected APP-CTFs bands A and B (lane WO2). (d) Immunoprecipitated APP-CTFs from the F2 fraction of the temporal cortex of a control (S0,c) and an AD patient (S9,c) were treated overnight with calf intestine alkaline phosphatase (+ CAP). APPCter-C17 antiserum detected three bands in the control samples at 13.5, 10.5 and 9.5 kDa. Note that in the AD sample the 13.5-kDa band is faintly detected whereas the 9.5-kDa band is intensively stained.

correspond either to unphosphorylated β′-stub or to incompletely dephosphorylated α-stub. Lower molecular weight APP-CTFs were not detected suggesting that the γ-stub (expected at 6.5 kDa) is not detected in our conditions.

Dephosphorylation of APP-CTFs was performed on brain tissue fraction F2 of the temporal cortex of control (S0,c) and the temporal cortex of an AD patient (S9,c). A lower level of band B and a higher level of band E was observed in AD (Fig. 4d). This result corroborated that obtained directly on fractions F2 (Fig. 4b, lanes 5, 7 and 9) and it suggested in addition a difference in the phosphorylation state of APP-CTFs in AD.

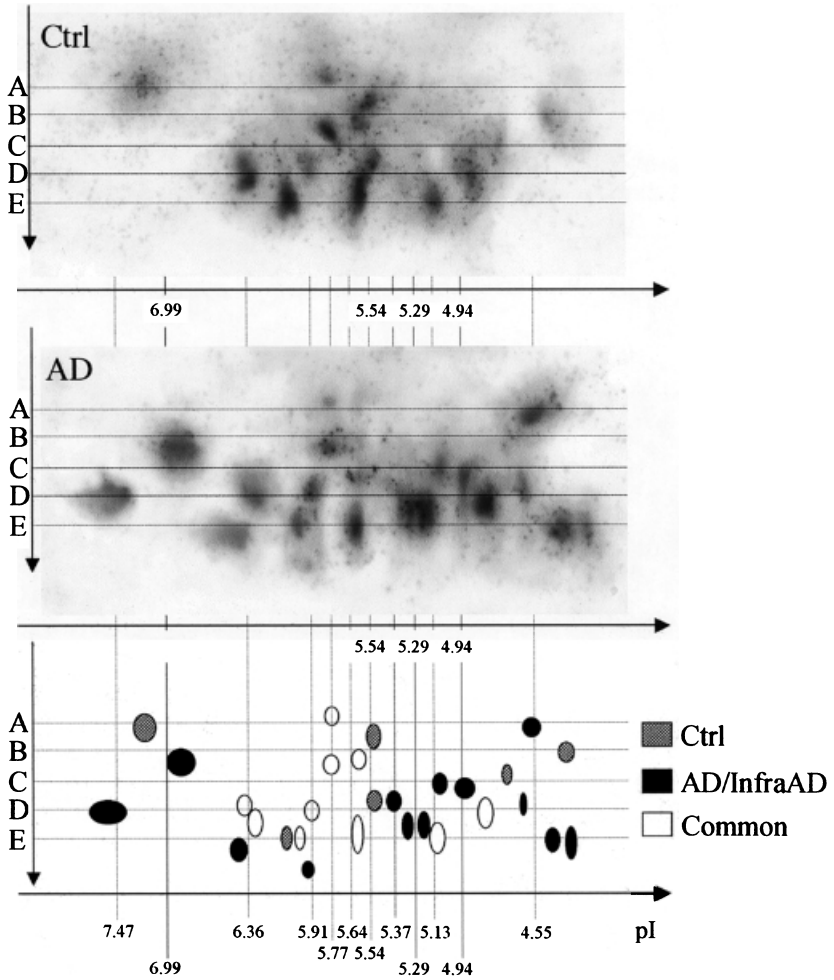

Fig. 5 Two-dimensional analysis of APP-CTFs in human brain APP-CTFs from the Triton-soluble fraction of control (Ctrl), infraclinical AD (infra-AD) and AD cases were resolved on a 3–10 immobilized pH gradient followed by Tris-Tricine SDS–PAGE and western blotting with APPCter-C17 antiserum. APP-CTFs bands (indicated A, B, C, D and E) were resolved in more than 15 individuals spots. The different APP-CTFs patterns were superposed and they are schematized on the third panel. Empty spots indicate the APP-CTFs common to Ctrl, infra-AD and AD. The hatched spots and the black spots correspond to APP-CTFs isovariants specifically detected in Ctrl and AD/infra-AD cases, respectively. Isoelectric points (pI) of APP-CTFs were determined using internal standards as α-enolase (pI of 6.99), γ-enolase (pI of 4.55) and cytoplasmic actin (5.29).

Post-translational modifications of APP-CTFs were investigated using two-dimensional gel electrophoresis coupled with western blotting. Analysis of APP-CTFs was performed in the F2 fraction of one control (S0,a), one infra-AD (S1,a) and one AD (S9,b) sample. Sixteen isovariants of APP-CTFs were detected in the control, whereas 23 isovariants were detected in AD (Fig. 5, Ctrl and AD panels). A synthesis of APP-CTFs patterns obtained from two-dimensional gel analyses of three cases is represented in Fig. 5 (third panel). This figure shows that nine isovariants of APP-CTFs spots are common to control, infra-AD and AD, six isovariants are only detected in control and 13 additional isovariants of APP-CTFs are detected in AD. These additional acidic isovariants corresponded mainly to APP-CTFs bands D and E, and they are consistent with the stronger staining of these bands on Tris-Tricine SDS–PAGE (Fig. 4b, case S9,b). Moreover, both dephosphorylation experiments and two-dimensional gel analysis suggest a higher degree of phosphorylation APP-CTFs band D and E in AD (Figs 4d and 5).

Discussion

APP dysfunction is the aetiologic factor of AD, as demonstrated by the pathological mutations on *APP*, *PS1* and *PS2* genes. These mutations provoke a degenerating process, an increased ratio of Aβ42 : Aβ40 peptides (except for the Swedish mutation) and amyloid plaques. Well correlated to dementia, tau pathology is also an inescapable and constant

event of FAD and non-FAD (Delacourte *et al*. 1999). Apart from these facts, we do not yet know precisely the origin of neurodegeneration. Aβ toxicity is frequently suggested, by indirect means, but either a loss of function of APP or a role of other metabolic products such as APP-CTFs can also be suggested (Neve 2001). In particular, it has been recently demonstrated that APP-CTFs bind to Fe65 to form an active transcriptional complex with Tip60 (Cao and Sudhof 2001). In the present study, our aim was to investigate whether APP-CTFs were significantly modified in AD. For that purpose, we analysed the qualitative and quantitative changes of APP-CTFs in the temporal and occipital brain areas of numerous patients at different stages of AD, from normal controls to severely affected patients. Our results demonstrate dramatic changes of APP-CTFs as a function of the progression of the disease, illustrated by the progressive extent of tau pathology in neocortical areas.

A significant decrease of APP-CTFs in AD

Using a western blot approach, we have been able to detect precisely and quantitatively the five (A–E) main bands that correspond to APP-CTFs in the human brain. A significant decrease was observed in non-FAD and FAD cases. Indeed, to explain the increase of Aβ production demonstrated well in FAD, an increase of APP-CTFs would have been expected. This is not the case, with the exception of one AD patient. Interestingly, the decrease was also observed at the infraclinical stages of AD. This general decrease was found evenly in two different neocortical brain areas, the temporal and occipital cortices.

It was also unexpected to have a global decrease of APP-CTFs in non-FAD patients as well as in some FAD cases, showing similar patterns of APP-CTFs. These data are in favour of a general dysmetabolism of APP-CTFs in all subtypes of AD. Intriguingly, only one case had a pattern opposite to all others, with huge quantities of APP-CTFs, but in agreement with the well known fact that this disease is extremely heterogeneous on many points, even those directly involved in the aetiology, as demonstrated by the numerous different mutations on APP and presenilin genes.

Characterization of APP-CTFs and modifications of their solubility distribution in AD

β-Stubs were selectively identified from β′-, α- or γ-stubs of APP-CTFs using WO2 antibody and we show that bands A, C and D correspond to phosphorylated variants of β-, β′- or α-stubs, because dephosphorylation of APP-CTFs result in the disappearance of corresponding bands. Our characterization is in agreement with that described by Russo *et al*. (2001) and also suggests that the recently described γ-stub or AICD (amyloid precursor protein intracellular domain) (Cupers *et al*. 2001; Kimberly *et al*. 2001; Sastre *et al*. 2001; Yu *et al*. 2001) is not a part of the five APP-CTFs bands described in human brain tissue.

Using a differential solubility assay, we show that in addition to reduced expression of APP-CTFs, α- and/or β′-stubs are present in higher levels in the Triton-soluble fraction, whereas β-stubs are present in higher levels in the SDS-insoluble fraction in AD. Moreover, dephosphorylation and two-dimensional analysis also suggest that α-stubs are phosphorylated more and, hence, it could account for their higher solubility. Conversely, the reduced solubility of β-stubs could be related to a reduced phosphorylation. Thus, our data suggest a relationship between the change of specific solubility, the progressive disappearance and post-translational modifications such as phosphorylation. This is illustrated by the presence of APP-CTFs isovariants that were only detected in the tissue affected by Alzheimerization, thus demonstrating a specific dysmetabolism of APP-CTFs in AD.

Conclusion

This is the first report demonstrating modifications of APP-CTFs in the human brain affected by AD. This demonstration was possible because we have a large bank of brain tissue that was carefully characterized at the clinical, neuropathological and biochemical levels. In particular with our biochemical approach we were able to differentiate clearly ageing from the infraclinical stages of AD, using a quantification of tau and Aβ pathologies in numerous brain areas. The staging of tau pathology was particularly helpful for grading the extent of Alzheimer pathology (Delacourte *et al*. 1999).

However, despite the complete characterization of the brain tissue used for our experiments, the APP-CTFs changes observed were not found in a precise and linear relationship with the other parameters of Alzheimer pathology. This is not surprising because AD is extremely heterogeneous, and is likely to be a disease resulting from a combination of numerous factors, each of them weighing more or less on the development of the pathology (Delacourte 2000). The statistical significance of APP-CTFs changes in AD demonstrated here is, however, very strong.

Two different hypotheses can explain our observations. First, loss of APP-CTFs could result from a modification of secretase activities, and especially from an activation of γ-secretases, and therefore a transformation of APP-CTFs into γ-CTFs, Aβ peptides and smaller fragments (see Fig. 1). The second hypothesis is that the targeting of APP in subcellular compartments is dys-regulated. The differential decrease of APP-CTFs in our differential solubility assay, and the different ratio between the five bands is in favour of such a hypothesis. The challenge to verify these hypotheses in relevant models remains.

Together, we demonstrate a dysfunction of APP that could be deleterious for neurones, and that could trigger tau pathology (Mesulam 1999; Delacourte 2000). One additional benefit of our study is that the precise modifications of

isovariants found in the nervous tissue in AD could be observed also in the peripheral fluids, as APP is an ubiquitous protein. If so, the decrease or the post-translational modification of APP-CTFs could be used as an early marker for the biological diagnosis of AD.

Acknowledgements

This work was supported by INSERM. We would like to thank Prof. Laquerierre from Rouen Hospital, for the gift of FAD brain tissue and Dr Bart de Strooper from Neuronal Cell Biology Laboratory, Flanders Institute for Biotechnology (VIB4) KU Leuven, Belgium for the gift of antibody B10 against APP-CTFs.

References

Allinquant B., Moya K. L., Bouillot C. and Prochiantz A. (1994) Amyloid precursor protein in cortical neurons: coexistence of two pools differentially distributed in axons and dendrites and association with cytoskeleton. *J. Neurosci.* **14**, 6842–6854.

Bouillot C., Prochiantz A., Rougon G. and Allinquant B. (1996) Axonal amyloid precursor protein expressed by neurons in vitro is present in a membrane fraction with caveolae-like properties. *J. Biol. Chem.* **271**, 7640–7644.

Campion D., Brice A., Dumanchin C., Puel M., Baulac M., De La Sayette V., Hannequin D., Duyckaerts C., Michon A., Martin C., Moreau V., Penet C., Martinez M., Clerget-Darpoux F., Agid Y. and Frebourg T. (1996) A novel presenilin 1 mutation resulting in familial Alzheimer's disease with an onset age of 29 years. *Neuroreport* **7**, 1582–1584.

Cao X. and Sudhof T. C. (2001) A transcriptively active complex of app with fe65 and histone acetyltransferase tip60. *Science* **293**, 115–120.

Cupers P., Orlans I., Craessaerts K., Annaert W. and De Strooper B. (2001) The amyloid precursor protein (APP)-cytoplasmic fragment generated by γ-secretase is rapidly degraded but distributes partially in a nuclear fraction of neurones in culture. *J. Neurochem.* **78**, 1168–1178.

De Strooper B. and Annaert W. (2000) Proteolytic processing and cell biological functions of the amyloid precursor protein. *J. Cell. Sci.* **113**, 1857–1870.

De Strooper B., Simons M., Multhaup G., Van Leuven F., Beyreuther K. and Dotti C. G. (1995) Production of intracellular amyloid-containing fragments in hippocampal neurons expressing human amyloid precursor protein and protection against amyloidogenesis by subtle amino acid substitutions in the rodent sequence. *EMBO J.* **14**, 4932–4938.

Delacourte A. (2000) Tau pathology: a marker of neurodegenerative disorders. *Curr. Opin. Neurol.* **13**, 371–376.

Delacourte A., David J. P., Sergeant N., Buee L., Wattez A., Vermersch P., Ghozali F., Fallet-Bianco C., Pasquier F., Lebert F., Petit H. and Di Menza C. (1999) The biochemical pathway of neurofibrillary degeneration in aging and Alzheimer's disease. *Neurology* **52**, 1158–1165.

Estus S., Golde T. E., Kunishita T., Blades D., Lowery D., Eisen M., Usiak M., Qu X. M., Tabira T., Greenberg B. D. *et al.* (1992) Potentially amyloidogenic, carboxyl-terminal derivatives of the amyloid protein precursor. *Science* **255**, 726–728.

Fassbender K., Simons M., Bergmann C., Stroick M., Lütjohann D., Keller P., Runz H., Kühl S., Bertsch T., Von Bergmann K., Nennerici M., Beyreuther K. and Hartmann T. (2001) Simvastin strongly reduces levels of Alzheimer's disease β-amyloid peptides Aβ42 and Aβ40 *in vitro* and *in vivo*. *Proc. Natl Acad. Sci. USA* **98**, 5856–5861.

Golde T. E., Estus S., Younkin L. H., Selkoe D. J. and Younkin S. G. (1992) Processing of the amyloid protein precursor to potentially amyloidogenic derivatives. *Science* **255**, 728–730.

Gorg A. (1993) Two-dimensional electrophoresis with immobilized pH gradients: current state. *Biochem. Soc. Trans.* **21**, 130–132.

Haass C., Schlossmacher M. G., Hung A. Y., Vigo-Pelfrey C., Mellon A., Ostaszewski B. L., Lieberburg I., Koo E. H., Schenk D., Teplow D. B. *et al.* (1992) Amyloid beta-peptide is produced by cultured cells during normal metabolism. *Nature* **359**, 322–325.

Hayashi H., Mizuno T., Michikawa M., Haass C. and Yanagisawa K. (2000) Amyloid precursor protein in unique cholesterol-rich microdomains different from caveolae-like domains. *Biochim. Biophys. Acta.* **1483**, 81–90.

Ida N., Hartmann T., Pantel J., Schröder J., Zerfass R., Förstl H., Sandbrink R. Masters C. L. and Beyreuther K. (1996) Analysis of Heterogeneous βA4 peptides in human cerebrospinal fluid and blood by a newly developed sensitive western blot assay. *J. Biol. Chem.* **271**, 22908–22914.

Ikezu T., Trapp B. D., Song K. S., Schlegel A., Lisanti M. P. and Okamoto T. (1998) Caveolae, plasma membrane microdomains for alpha-secretase-mediated processing of the amyloid precursor protein. *J. Biol. Chem.* **273**, 10485–10495.

Kimberly W. T., Zheng J. B., Guénette S. Y. and Selkoe D. J. (2001) The intracellular domain of the β-amyloid protein is stabilized by Fe65 and translocates to the nucleus in a Notch-Like manner. *J. Biol. Chem.* **276**, 40288–40292.

LeBlanc A. (1994) The role of beta-amyloid peptide in Alzheimer's disease. *Metab. Brain. Dis.* **9**, 3–31.

Mesulam M. M. (1999) Neuroplasticity failure in Alzheimer's disease: bridging the gap between plaques and tangles. *Neuron* **24**, 521–529.

Neve R. L. (2001) A beta may be a planet, but APP is central. *Neurobiol. Aging* **22**, 151–154.

Neve R. L., McPhie D. L. and Chen Y. (2000) Alzheimer's disease: a dysfunction of the amyloid precursor protein. *Brain Res.* **886**, 54–66.

Russo C., Salis S., Dolcini V., Venezia V., Song X., Teller J. K. and Schettini G. (2001) Identification of Amino-Terminally and Phosphotyrosine-Modified Carboxy-Terminal Fragments of the Amyloid Precursor Protein in Alzheimer's Disease and Down's Syndrome Brain. *Neurobiol. Dis.* **8**, 173–180.

Sastre M., Steiner H., Fuchs K., Capell A., Multhaup G., Condron M. M., Teplow D. B. and Haass C. (2001) Presenilin-dependent γ-secretase of β-amyloid precursor protein at a site corresponding to the S3 cleavage of Notch. *EMBO Reports* **21**, 1–7.

Schägger H. and von Jagow G. (1987) Tricine-sodium dodecyl sulfate-polyacrylamide gel electrophoresis for the separation of proteins in the range from 1 to 100 kDa. *Anal. Biochem.* **166**, 368–379.

Suh Y. H. (1997) An etiological role of amyloidogenic carboxyl-terminal fragments of the beta-amyloid precursor protein in Alzheimer's disease. *J. Neurochem.* **68**, 1781–1791.

Westermeier R., Postel W., Weser J. and Gorg A. (1983) High-resolution two-dimensional electrophoresis with isoelectric focusing in immobilized pH gradients. *J. Biochem. Biophys. Meth.* **8**, 321–330.

Yu C., Kim S. H., Ikeuchi T., Xu H., Gasparini L., Wang R. and Sisodia S. S. (2001) Characterization of a presenilin-mediated APP carboxyl terminal fragment γCTFγ: Evidence for distinct mechanisms involved in γ-secretase processing of the APP and notch 1 transmembrane domains. *J. Biol. Chem.* in press.